JET–P(99)18

G D Conway et al

Suppression of Plasma Turbulence during Optimised Shear Configurations in JET

JET–P(99)18

Suppression of Plasma Turbulence during Optimised Shear Configurations in JET

G D Conway, D N Borba, B Alper, D V Bartlett,
C Gormezano, M G von Hellermann, A C Maas,
V V Parail, P Smeulders, K-D Zastrow.

JET Joint Undertaking, Abingdon, Oxfordshire, OX14 3EA,

Preprint of a Paper to be submitted for publication in Physical Review Letters

August 1999

ABSTRACT

Density turbulence suppression is observed in the internal transport barrier (ITB) region of JET discharges with optimised magnetic shear. The suppression occurs in two stages. First, low frequency turbulence is reduced across the plasma core by a toroidal velocity shear generated by intense auxiliary heating. Then when the ITB forms, high frequency turbulence is reduced locally within the steep pressure gradient region of the ITB, consistent with the effects of enhanced $E \times B$ poloidal shear. The turbulence suppression is correlated with reduced plasma transport and improved fusion performance.

Much effort has been spent in recent years in developing alternative scenarios for operating tokamak fusion reactors. One particular scenario involves reversing or reducing the central magnetic shear to form an internal transport barrier (ITB). The result is reduced plasma core energy transport and enhanced fusion performance [1-7]. It is believed that ITBs may be formed through a combination of $E \times B$ velocity shear and magnetic shear stabilisation of plasma turbulence and instabilities [8].

In this Letter we present results from JET optimised shear discharges [5] showing that turbulence suppression during ITB formation occurs in two stages. First low frequency turbulence is reduced across the plasma core, coinciding with a region of strong toroidal velocity shear; then high frequency turbulence is locally suppressed around the ITB region, consistent with enhanced pressure gradient driven $E \times B$ poloidal shear.

The measurements were made using a system of X-mode reflectometers consisting of two, dual-channel toroidal correlation reflectometers at 75GHz (covering plasma outboard edge) and 105GHz (core & inboard edge), and a 92-96GHz swept frequency radial correlation reflectometer (plasma core) [9]. Reflectometry is a powerful tool for measuring density fluctuations. The highly localised reflection of the microwave beam gives excellent spatial localisation. Measurements can be made throughout the plasma as the radial location of the cutoff layer depends on the launched microwave frequency, the toroidal magnetic field B_T, plasma current I_p, and plasma density n_e. Reflectometers are primarily sensitive to long wavelength transverse fluctuations, i.e. wavelengths greater than the beam radius w. For the JET reflectometers the w~5cm and so are predominately sensitive to wavenumbers $k_\perp < 1.2\text{cm}^{-1}$.

Spatially, the turbulence in optimised shear discharges can be separated into three regions: outside the ITB (edge), within the ITB gradient, and inside the ITB (core). The turbulence behaves differently in each region. The core turbulence (ITB & within) evolves through four distinct phases. (1) Ohmic breakdown. (2) L-mode pre-heat, using Ion Cyclotron Resonance Heating (ICRH) to slow the current penetration and control the q profile evolution. (3) Main heating using combined co-injected (parallel to I_p) Neutral Beam Injection (NBI) and ICRH, and (4) the ITB formation. The edge turbulence by contrast shows little variation as the discharge evolves.

Figure 1 shows time traces of typical plasma parameters from a $B_T \approx 3.4$T, $I_p \approx 3.4$MA (peak), optimised shear discharge #46727. This discharge was selected to illustrate the behaviour of the turbulence for two reasons. (1) The formation of the ITB is delayed by almost one second due to the uneven coupling of the ICRH power (keeping the input heating power below the ITB threshold), allowing the effects of the ITB to be clearly separated from those due to the NBI. (2) During the ITB phase a reflectometer cutoff layer (92GHz) is located within the ITB gradient region.

Figure 2 shows the spectral evolution of the core turbulence measured with this 92GHz reflectometer channel. The spectrogram begins with the ICRH pre-heat phase, at 3.5s into the

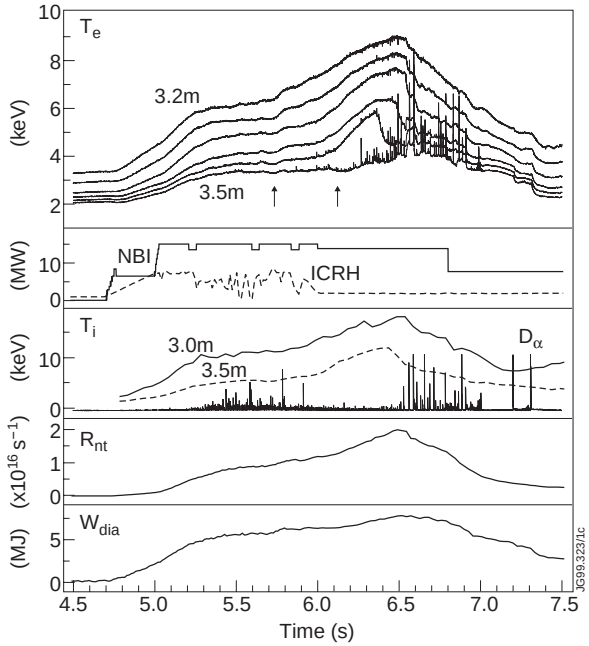

Fig.1: Time traces of (a) electron temperature at various radial locations (b) NBI and ICRH power (c) $D\alpha$ *emission and* T_i *at core & mid-radius (d) neutron rate* R_{nt} *and (e) stored energy* W_{dia} *for shot #46727.*

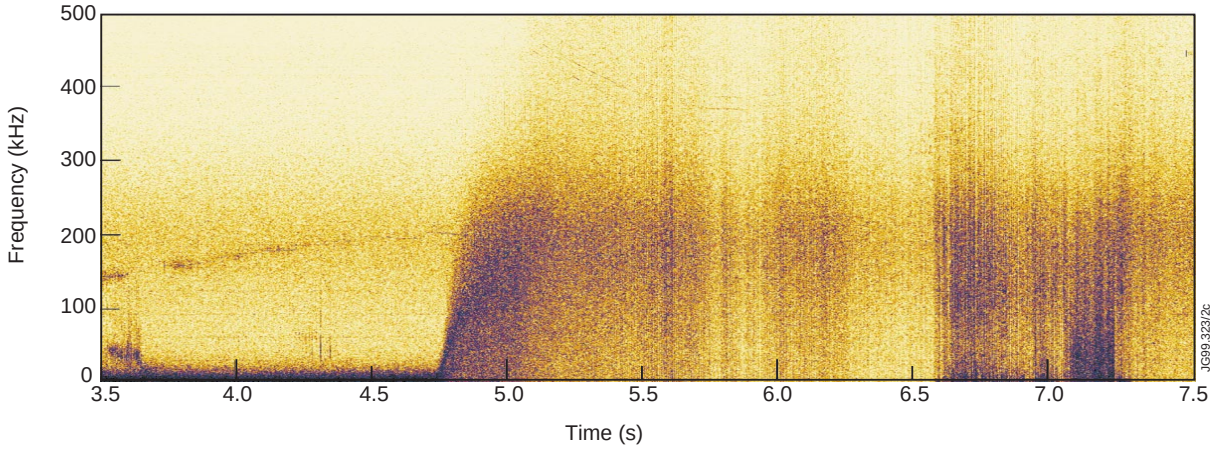

Fig.2: Spectrogram (log intensity) of density fluctuations ($A\cos\phi$*) from a 92GHz reflectometer channel (*$R \approx 3.2$ *- 3.6m) for shot #46727. n.b. slight background feature around 200kHz due to amplifier gain anomaly.*

discharge. The spectrum is dominated by large amplitude low frequency turbulence ($f < 50$kHz). The turbulence is ballooning in character with amplitudes 10 or more times higher in the outboard edge compared to the inboard edge. The low ICRH power (2MW) has little effect on the core or edge turbulence compared to the preceding ohmic phase. However its main effect is to generate large amplitude core localised Toroidal Alfven Eigenmodes between 100 to 200kHz together with lower frequency modes around 20kHz. Figure 3 shows another example (complex amplitude $Aexp(i\phi)$) with spectra from a 75GHz reflectometer channel during ohmic, ICRH and NBI phases of a $B_T \approx 2.5$T, $I_p \approx 2.5$MA discharge (#46437) as the cutoff layer moves from the

core, through the ITB at $R \approx 3.65$m, to the outboard edge. The spike at zero frequency is the reflectometer carrier wave and indicates the level of reflected power.

The main part of the discharge in Fig.2 begins at 4.7s with the high power heating phase, consisting of combined NBI and ICRH with a total power of >15MW. The power is usually stepped up in two stages to delay the formation of an H-mode during the I_p ramp. The spectrogram shows a sudden transformation in the core turbulence. The spectrum rapidly broadens with frequencies spreading up to $f >$ 300kHz followed by a complete suppression of low frequency turbulence, c.f. Fig.3(c). Note that the level of high frequency turbulence increases throughout the plasma (edge as well as core) scaling with heating power.

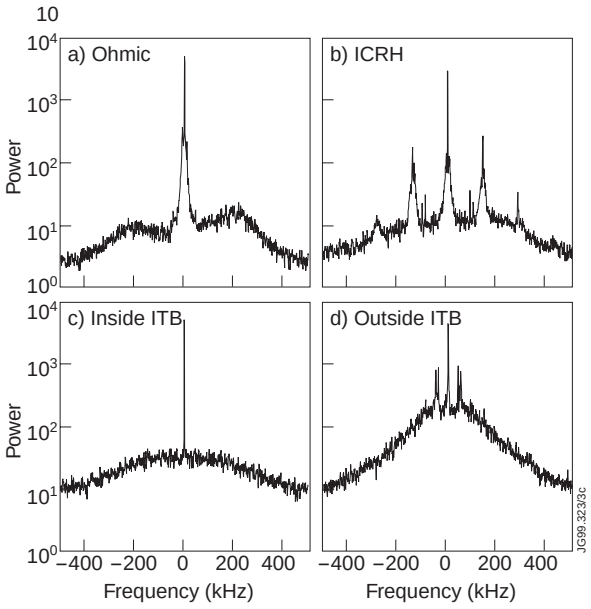

Fig.3: Spectra from 75GHz reflectometer channel (Aexp(iϕ) signal) as cutoff layer moves outwards during 2.5T shot #46437; (a) ohmic: R ≈ *3.2m, (b) ICRH:* R ≈ *3.2m, (c) inside ITB:* R ≈ *3.5m, (d) outside ITB:* R ≈ *3.8m*

This is the point in the discharge (5.0 to 5.2s) where an internal transport barrier would normally form - provided the q profile (and magnetic shear) has evolved correctly and sufficient heating power is applied. However because of the uneven ICRH power matching the ITB does not form until 6.2s, and then only lasts until 6.5s when it is terminated by a plasma instability (q = 2 snake). At precisely these two times the spectrogram shows an extremely fast collapse and recovery in the high frequency turbulence. There is also a similar drop in high frequency turbulence at 5.7s coinciding with a sudden rise in the core T_e and T_i (and hence pressure gradient ∇P) and increases in the neutron rate R_{nt} and plasma stored energy W_{dia}, Fig.1. This might have been the early stage of an ITB but it was not sustained; T_e rises at the edge around 5.9s and ∇P is reduced.

Although shot #46727 is slightly atypical with its delayed ITB, it clearly illustrates the two distinct stages in the reduction of turbulence. The individual features are observed in all JET optimised shear discharges. However the turbulence suppression is by no means global. Lower B_T discharges with strong I_p ramping (such as #46437 in Fig.3) where the reflectometer cutoff layers are swept across the plasma through the ITB region reveal: (1) The initial low frequency suppression occurs right across the core out to the ITB foot. (2) The high frequency suppression is restricted to the narrow ITB gradient region.

This gradient region is illustrated with the electron temperature T_e (from ECE) and ion temperature T_i (from CXS) profiles in Fig.4 during the ITB phase of shot #46727. Both T_e and T_i show steep gradients with foot-points which coincide and track each other as the ITB expands

and contracts. The main difference though is that T_i peaks at the magnetic axis while the T_e profile flattens towards the core. The gradient foot also tracks a boundary in the toroidal rotation. Fig.5 is a contour plot of toroidal rotation frequency ω_{rot} (from CXS) against major radius and time for shot #46727. As soon as the main heating is applied the plasma core begins to spin-up toroidally (driven by pressure gradient and/or momentum injection), then levels off until the formation of the ITB after 6.0s. The edge plasma remains virtually stationary throughout the heating phase (confirmed by reflectometer measurements of turbulence propagation velocities of $v < 10\text{kms}^{-1}$). This generates two regions, one of low velocity shear in the edge and one of high velocity shear across the core. The boundary (indicated by the change in spacing of the contours) expands and contracts during the heating phase and coincides with the foot of the temperature gradient (marked with crosses). Since the high shearing region is semi-global (e.g. half minor radius or more) it may be expected to primarily affect fluctuations of similar scale lengths, i.e. long wavelengths.

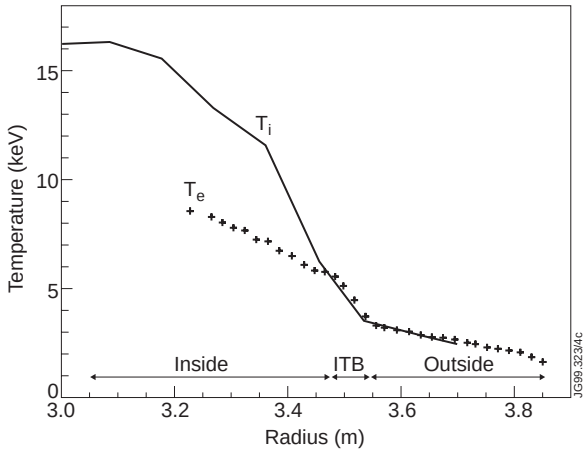

Fig.4: Radial electron & ion temperature profiles (from a 48 channel heterodyne ECE radiometer and CXS) at 6.28s during shot #46727.

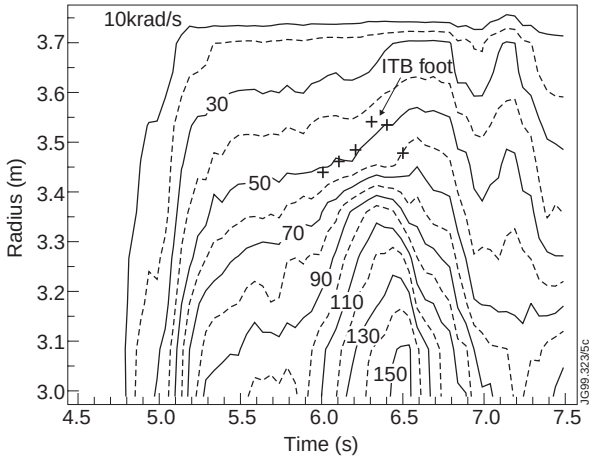

Fig.5: Contour plot of toroidal angular rotation frequency ω_{rot} from charge exchange spectroscopy vs radius and time for shot #46727. Crosses mark position of ITB 'foot' from the T_e *profile.*

In the ohmic/L-mode phase reflectometer dispersion relation measurements show that the turbulence is dominated by long wavelengths $K_\perp\rho_i<<1$. This is also confirmed by mode analysis of magnetic signals which show only low toroidal n (e.g. 0, 1, and 2) coherent fluctuations, while the NBI/ICRH phase contains only high $n > 10$ fluctuations, i.e. short wavelength $K_\perp\rho_i\sim1$. One explanation is that the velocity shear breaks up the long wavelength turbulence into shorter wavelengths, or that it prevents the normal dissipation/cascade of energy between short and long wavelengths.

This hypothesis that toroidal velocity shear suppresses long wavelengths is also supported by observations of turbulence behaviour during other types of discharges. Edge turbulence is reduced during Hot ion H-modes when a strong toroidal velocity shear forms at the H-mode pedestal. But during ELMy H-mode discharges this velocity shear is destroyed by the ELMs

(Edge Localised Modes) and low frequency edge turbulence is actually enhanced. This is the same situation in the stationary edge region of ITB discharges. The edge turbulence remains high throughout the discharge. If the discharge maintains an L-mode like edge then the turbulence spectrum is narrow with an exponential shape, while for an ELMy H-mode edge pedestal the spectrum is broader with a bell-shape and strong MHD, Fig.3(d).

Figures 1 and 2 show that the level of turbulence is related to the fusion performance. The turbulence also appears to be linked with local values of plasma transport. The periods of reduced high frequency turbulence coincide with periods of localised increased electron and ion pressure gradients ∇P_e and ∇P_i at the ITB. This, together with the fast transitions in the turbulence level, suggests a positive feedback loop [8] in which an increase in the pressure gradient leads to an increase in the poloidal $E \times B$ shear, which locally suppresses turbulence (with scale lengths comparable to the ∇P width, i.e. cm wavelengths) which in turn leads to improved confinement and fusion performance, and hence a further increase in ∇P. It must be stressed that discharges without ITBs show no high frequency reduction. Further, the level of the high frequency turbulence is correlated with the T_e gradient. The flattening of the T_e profile in the core, Fig.4, results in electron thermal conductivity χ_e (from TRANSP analysis) dipping at barrier and then rising again slightly in the core [6]. That is there is a link between the local χ_e value (at the ITB) and the level of short wavelength fluctuations. A similar link has also been observed in TFTR plasmas with enhanced reversed shear [10]. Conversely the suppression of long wavelength fluctuations is correlated with the ion thermal conductivity χ_i. The peaked T_i profile (i.e. constant or rising ∇P_i between the barrier 'foot' and the core) results in the toroidal rotation increasing towards the core, and χ_i dropping towards neo-classical values at barrier, then staying low throughout the core.

Improvements in plasma confinement are also accompanied by reductions in turbulent correlation lengths. Reflectometer measurements in the core show a dramatic collapse in the low frequency toroidal coherence, Fig.6, between the L-mode and main heating phases. Due to the inclination of the magnetic field lines this actually indicates a reduction in the perpendicular correlation length. Measurements of radial correlation lengths are more difficult due to low levels of signal correlation. Nevertheless they indicate radial correlation lengths in the core of only a few mm's. These measurements however are not inconsistent with a picture of large-scale perturbations with poloidally spiralling structures obtained by several authors (e.g. Ref.[11]) using numerical simulations. These structures, while maintaining long spiralling connection lengths, can have narrow radial

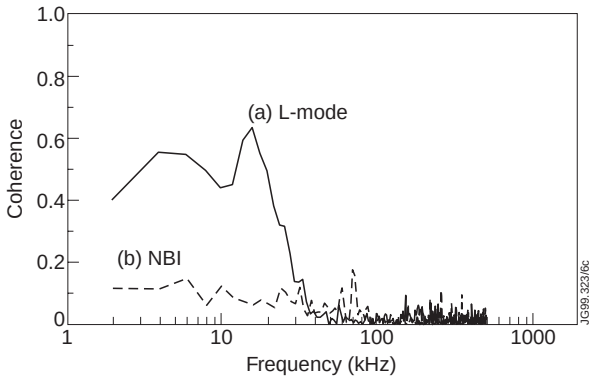

Fig.6: Coherence spectra between two toroidally separated reflectometer channels (40mm) during (a) L-mode: $R \approx 3.2m$, *and (b) NBI/ICRH:* $R \approx 3.5m$ *phases of shot #46423.*

widths and hence appear to have short instantaneous radial correlation lengths. Velocity shearing could break up these spirals into smaller segments and hence reduce cross-field transport.

To summarise, our results show : (1) The formation of a core region of high radial shear in the plasma toroidal velocity (induced by high power NBI and ICRH) is correlated with the suppression of long wavelength turbulence, and with a decrease in the ion thermal conductivity χ_i. (2) The subsequent formation of an internal transport barrier is correlated with a localised suppression of shorter wavelength turbulence and a coincident localised drop in the electron thermal conductivity χ_e. The behaviour of the turbulence suppression is consistent with the effects of a positive feedback loop involving $E \times B$ shear. For the long wavelength suppression the toroidal velocity appears to be the dominant term, while for the shorter wavelengths the ∇P_i term may be more significant. These results present a coherent picture showing the importance of short and long wavelength turbulence and its link to the formation of internal transport barriers and the subsequent performance of the discharge.

ACKNOWLEDGEMENTS

We would like to acknowledge A.Fasoli, R.C.Felton, D.Testa and R.F.Heeter for assistance with data acquisition, A.Thyagaraja for useful discussions, and members of Task Force B and JET Team for the operation of the JET tokamak.

REFERENCES

[1] E.J.Synakowski, Plasma Phys. Control. Fusion **40**, 581 (1998).
[2] L.L.Lao *et al*., Phys. Plasmas **3**, 1951 (1996).
[3] C.L.Rettig *et al*., Plasma Phys. Control. Fusion **40**, 811 (1998).
[4] E.Mazzuccato *et al*., Phys. Rev. Lett. **77**, 3145 (1996).
[5] C.Gormezano *et al*., Phys. Rev. Lett. **80**, 5544 (1998).
[6] X.Litaudon *et al*., Plasma Phys. Control. Fusion **41**, A733 (1999).
[7] T.Fujita *et al*., Phys. Rev. Lett. **78**, 2377 (1997).
[8] K.H.Burrell, Phys. Plasmas **4**, 1499 (1997).
[9] G.D.Conway, G.Vayakis, J.A.Fessey and D.V.Bartlett, Rev. Sci. Instrum. (1999). Oct. (Inpress)
[10] K.L.Wong *et al*., Phys. Lett. A **236**, 339 (1997).
[11] Y.Kishimoto *et al*., Plasma Phys. Control. Fusion **41**, A663 (1999).